Actin Polymerization State Regulates Osteogenic Differentiation in Human Adipose-derived Stem Cells

Bing Sun
Southern Medical University
Xin Jiang
Southern Medical University
Rongmei Qu
Southern Medical University
Tingyu Fan
Southern Medical University
Yuchao Yang
Southern Medical University
Asmat Ullah Khan
Southern Medical University
Zhitao Zhou
Southern Medical University
Jun Ouyang
Southern Medical University
jingxing dai (daijx2013@163.com)
southern meidcal university https://orcid.org/0000-0002-9339-9174

Research

Keywords: human adipose-derived stem cells, actinpolymerization, osteogenic differentiation, jasplakinolide, cell proliferation and migration

DOI: https://doi.org/10.21203/rs.3.rs-33693/v1

Abstract

Background: Actin is an essential cellular protein that assembles into microfilaments and regulates numerous processes such as cell migration, maintenance of cell shape, and material transport. In this study, we explored the effect of actin polymerization state on the osteogenic differentiation of human adipose-derived stem cells (hASCs).

Methods: The hASCs were treated with different concentrations (0, 1, 5, 10, 20, and 50 nM)of jasplakinolide (JAS), a reagent that directly polymerizes F-actin.The effects ofthe actin polymerization state on cell proliferation, apoptosis, migration, and the maturity of focal adhesion-related proteins were assessed. In addition, western blotting and alizarin red staining assays were performed to assess osteogenic differentiation.

Results: These results revealed that cell proliferation and migration in the JAS (0, 1, 5, 10, and 20 nM) groupswashigher than that inthe control group andthe JAS (50 nM) group.The protein expressionof focal adhesion kinase, vinculin, paxillin, and talinwere highest in the JAS (20 nM) group, whilezyxin expression was highestinthe JAS (50 nM) group.Western blottingshowed thatosteogenic differentiation in theJAS (0, 1, 5, 10, 20, and 50 nM) groupswas enhanced compared with that in thecontrol group, and was strongest inthe JAS (50 nM) group.

Conclusions: Our data suggest thatthe actinpolymerization state may promote the osteogenic differentiation of hASCs by regulating the protein expression of focal adhesion-associated proteins in a concentration-dependent manner. Our findings provide valuable information for exploring the mechanism of osteogenic differentiationin hASCs.

Introduction

Actin, a single polypeptide chain globular protein with a molecular weight of 42kD, is the primary component of the cytoskeleton. There are two main forms of actin, the globular actin monomers (G-actin) and the polymeric actin filaments (F-actin). Actin plays a crucial role in many biological systems. The polymerization/depolymerization of actin is closely related to numerous cell activities, including the maintenance of cell morphology [1], cell movement [2], cytoplasmic streaming [3], material transport, apical growth, physical, and chemical signal transduction [4–7]. The dynamic remodeling of F-actin plays a crucial role in many diseases, such as cancer and malaria, and is additionally involved in the wound healing process, embryonic development, and tissue formation [8, 9].

In recent decades, several substances involved in the regulation of actin polymerization and depolymerization have been investigated. These include phalloidin [10], cytochalasin D [11], and latrunculin A, which can alter intracellular actin organization [12]. This group also includes jasplakinolide (JAS) / jaspamide [13–16] which was originally isolated from marine sponge [17–20]. A major advantage of JAS is that it is membrane permeable [21], which makes it an ideal tool for stabilizing or polymerizing actin filaments in live cells. It induces the nucleation of actin filaments, reduces the rate of

dissociation of actin subunits from F-actin filaments, and prevents cofilin from G-actin, resulting in filament stabilization [20, 22, 23].

Adipose-derived stem cells are a type of adult mesenchymal stem cell derived from fat tissue. They self-replicate and can differentiate in multiple directions [24–27], including the osteogenic, adipogenic [27–29], chondrogenic [30], and myogenic [29, 31] routes. ASCs are a good cell source for stem cell research [26] because they are widely available, easy to isolate, proliferate stably *in vitro*, and have a low decay rate [27, 32, 33]. Numerous studies have demonstrated that the polymerization of the actin cytoskeleton can affect cell migration, proliferation, and differentiation [2, 34]. Recent studies have shown that actin microfilament expression increased during the process of osteogenic differentiation. These microfilaments are orderly, thick, and arranged in a filamentous shape[12]. However, how osteogenic differentiation is affected by the extent of actin filament polymerization remains unclear. Therefore, in our study, human adipose-derived stem cells (hASCs) were treated with different concentrations of JAS (resulting in different degrees of polymerization) to study the influence of actin polymerization state on the osteogenic differentiation of hASCs.

Results

1. The effect of different actin polymerization states on the proliferation of hASCs

We evaluated the effects of different polymerization states of actin on the proliferation of hASCs. Here, we performed both Ki67 immunofluorescence staining and CCK-8 experiments. The results revealed that the cell proliferation rate in the JAS (1, 5, 10, 20, and 50 nM) groups was higher than that in the control; furthermore, it gradually increased with the increasing JAS concentrations, but significantly decreased in the JAS (50 nM) group ($p < 0.05$, Fig. 1A). The Cell Counting Kit-8 (CCK-8) result and cell counter assay were consistent with Ki67 results (Fig. 1B, C). These findings suggest that the actin polymerization caused by JAS at the lower concentration range (1–20 nM) promoted cell proliferation, while the high concentrations JAS (50 nM) inhibited it.

2. hASCs apoptosis and its relationship to actin polymerization state

To investigate the effects of different actin polymerization states on cell apoptosis, we performed the Annexin V-FITC/PI apoptosis assay. Flow cytometry results confirmed that the cell apoptosis rates of the JAS (1, 5, 10, and 20 nM) groups were lower than that of the control group. In contrast to this, the cell apoptosis rate in the JAS (50 nM) group was markedly increased (0.879%) (Fig. 2A), indicating that a high concentration of JAS promoted cell apoptosis.

3. The influence of different actin aggregation states on hASCs migration

Previous research has demonstrated that the state of actin filaments can regulate cell movement [35]. To study the effect of different polymerization states of actin on cell migration, we conducted wound healing and transwell experiments, respectively. The wound healing results suggested that the healing speed in the JAS (1, 5, 10, and 20 nM) groups was faster than that of the control group, while the JAS (50 nM) group was slower than the control group (Fig. 3A). Transwell results (Fig. 3B) showed that in the JAS (1, 5, 10, and 20 nM) groups, the number of cells in the lower chamber gradually increased but decreased sharply in the JAS (50 nM) group (which was significantly lower than the control group). Transwell results were generally consistent with the wound healing results. This data demonstrated that actin polymerization induced by a low concentration of JAS is beneficial for increasing cell migration. In contrast, a high concentration of JAS induced actin polymerization and negatively regulated cell migration.

4. Different actin polymerization states and the maturity of focal adhesions

Studies have shown that the dynamic changes of integrins and focal adhesions are involved in cell migration [35]. Therefore, we hypothesize that the different polymerization states of actin result in differences in cell migration because actin polymerization affects the maturity of focal adhesions. To confirm this, we used western blot analysis to detect the protein expression level of focal adhesion-related proteins (focal adhesion kinase (FAK), vinculin, talin, paxillin, and zyxin). The results showed that β-actin, FAK, vinculin, talin, and paxillin were all highly expressed in JAS (1, 5, 10, 20 and 50 nM) groups, but they were highest in the JAS (20 nM) group, and then subsequently decreased in the JAS (50 nM) group. However, interestingly, the expression of β-actin and zyxin showed a continuous increase in the JAS (1, 5, 10, 20, and 50 nM) groups, but there was no decrease in the JAS (50 nM) group (Fig. 4A, B). Therefore, we believe that actin polymerization could influence the maturity of focal adhesions and that there may be a difference between the influence of low and high actin polymerization states.

5. Actin polymerization can promote the localization of yes associated protein (YAP) to the cytoplasm

According to the literature, actin depolymerization can induce the nuclear localization of YAP and regulate gene expression [36–38]. Therefore, we speculated that different polymerization states of actin might have different effects on the nuclear localization of the YAP protein. To verify this, we used immunofluorescence staining to detect the changes in YAP localization. Results revealed that YAP was mainly concentrated in the nucleus in the control group, but that it began to diffuse into the cytoplasm after cells were treated with JAS. The higher the concentration of JAS, the more apparent the YAP cytoplasmic localization (Fig. 5A). We also verified this at the protein expression level. The expression of YAP and p-YAP (Ser127) in the JAS (1, 5, 10, 20, and 50 nM) groups was higher than that in the control

group (Fig. 5B, C). As the concentration of JAS increased, the ratio of p-YAP to YAP also increased. These data demonstrated that actin polymerization might potently activate YAP by inducing phosphorylation and cytoplasm localization.

6. The effects of different actin polymerization states on alkaline phosphatase (ALP) activity in hASCs

Actin polymerization and depolymerization are involved in the regulation of cell differentiation and other biological processes [12]. We believe that JAS may guide the differentiation of cells into osteoblasts. ALP staining and ALP activity assays were performed to explore the effect of actin polymerization on ALP activity in hASCs. The ALP staining results showed that positive staining gradually increased with increasing concentrations of JAS, from 0 nM to 20 nM; however, at the concentration of 50 nM, ALP activity was inhibited (Fig. 6A). The results of the ALP activity assay were approximately consistent with the results of ALP staining (Fig. 6B). Therefore, our results demonstrate that actin polymerization leads to an increase in ALP activity and content, which can influence cell fate, and subsequently, direct cells towards an osteogenic lineage.

7. Actin polymerization state and osteogenic differentiation of hASCs

The influence of different actin polymerization states on the osteogenic ability of hASCs was investigated by treating the cells with osteogenic induction medium (OS) containing different concentrations of JAS. The alizarin red assay showed that the positive staining in the JAS (1, 5, 10, 20 and 50 nM) groups was higher than that in the control group and strongest in the JAS (50 nM) group (Fig. 7A). Western blotting results demonstrated that osteogenic differentiation markers, such as osteopontin (OPN) and runt-related transcription factor 2 (RUNX2), were highly expressed in the JAS (1, 5, 10, 20, and 50 nM) groups compared with that in the control group (Fig. 7B). These results suggest that JAS may stimulate the osteogenic differentiation of hASCs in a concentration-dependent manner.

Discussion

In this study, we used different concentrations of JAS (an actin polymerization agent) to determine the effects of varying actin polymerization states on the osteogenic differentiation of hASCs. These results, including CCK-8, Ki67 immunofluorescence staining, cell apoptosis, wound healing, and the transwell assay, showed that JAS could promote cell proliferation and migration within a specific concentration range. These data indicated that in the JAS (50 nM) group, cell survival rate, cell proliferation, and migration significantly decreased, while the osteogenic differentiation ability increased. Therefore, we concluded that the polymerization of actin might trigger some osteogenesis-related signaling pathways. These results revealed that the low states of actin polymerization promoted cell proliferation and that

high states induced cell apoptosis. This may be due, in part, to JAS cytotoxicity at high concentrations, and the subsequent triggering of downstream signaling pathways related to cell apoptosis.

Cell migration depends on the activity of integrins and the maturation of focal adhesions. According to these findings, the different actin polymerization states resulted in varying focal adhesion maturity (Fig. 4A, B). It is noteworthy that the expression level of zyxin did not decrease at JAS (50 nM), but continued to increase. This trend is consistent with the osteogenic differentiation ability of cells in the OS + JAS (50 nM) group (Fig. 7A, B). Therefore, zyxin, a member of the focal adhesion, may be a key role for F-actin to regulate the osteogenic differentiation of cells. In the follow-up research project, we will focus on this key protein (zyxin). Additionally, under the action of a high concentration of JAS (50 nM), the mechanism of the decrease of partial adhesion-related protein expression is still unclear, and further research is urgently needed.

Osteogenic differentiation of hASCs is a complex process in which multiple genes, proteins, and signaling pathways interact with each other [39–41]. The reorganization of the actin cytoskeleton plays an essential role during stem cell differentiation. Previous work has shown that both the location and polymerization of cellular actin aids in the regulation of differentiation. The formation of actin stress fibers is essential for osteogenesis, while its inhibition stimulates lipogenesis [42].

Conclusion

In summary, in this study, we treated hASCs with different concentrations of JAS to maintain actin in specific polymerization states. We found that increased polymerization of actin promoted osteogenic differentiation, and this may have been achieved by regulating the focal adhesion-related proteins involved in activating YAP. This work forms the basis for further exploration of the mechanisms underlying the osteogenic differentiation of human adipose-derived stem cells.

Materials And Methods

Cell culture and jasplakinolide assay

Human fat tissue was washed with phosphate-buffered saline (PBS) three times, cut into a chyle shape, and then incubated in 0.15% collagenase type I (Sigma, NY, USA) at 37 °C, 5% CO_2 for 60 min. An equal volume of growth medium containing 10% FBS (Gibco, NY, USA) and 1% Penicillin-Streptomycin (Gibco, NY, USA)) was used to terminate digestion. This mixture was centrifuged for 5 min at 250 g (room temperature), the supernatant was removed, and the pellet was suspended in growth medium and incubated at 37 °C, 5% CO_2. After 24 h, the medium was completely replaced with fresh medium, and subsequently changed every other day. The cells were passaged at 80% confluence and used between the 3rd -5th passage (plating density = 6,000 cells/cm^2). After 24 h, cells were treated daily with a growth medium containing different concentrations of Jasplakinolide, or control medium containing the same volume of Dimethyl sulfoxide (DMSO).

Cell Counting Kit-8 (CCK-8) assay

Cells were washed three times with PBS, then incubated with CCK-8 solution (Dojindo Cell Counting Kit-8) according to the manufacturer's instructions (37 °C, 5% CO_2 incubator). After 0.5 h, absorbance was measured at 540 nm using a microplate reader (Bio-Rad, USA).

Immunofluorescence assay

Cells were washed two or three times with PBS, then fixed in 4% paraformaldehyde for 10 min, washed three times with PBS, and permeabilized with 0.1% Triton X-100 for 5 min, and blocked in 2% BSA for 1 h at room temperature. Next, cells were incubated with primary antibodies (FAK, 1:500, Cell Signaling Technology, USA; Talin, 1:500, Millipore, USA; Vinculin, 1:1000, Sigma-Aldrich, USA; Paxillin, 1:500, Becton Dickinson, USA; Zyxin, 1:500, Affinity, USA) overnight at 4 °C. The corresponding secondary antibody was then added to samples and incubated at room temperature for 1 h. These antibodies included Cy3 labeled goat anti-rabbit IgG (H + L), Beyotime, China; Alexa Fluor® 546 goat anti-mouse, Life Technologies, USA; or Alexa Fluor™ 488 phalloidin, Thermo Fisher Scientific, USA. After washing three times with PBS, cells were incubated with DAPI. The images were observed and captured using a fluorescence microscope (Carl Zeiss; German). Data analysis was performed using ImageJ 1.52V (NIH, USA).

Cell apoptosis

Cells were washed three times with PBS and digested with trypsin (without EDTA). Then cells were recovered by centrifugation (500 g for 5 min), washed with pre-cooled PBS, and then centrifuged again (500 g for 5 min). To measure apoptosis, we used the Annexin V-FITC/Propidium Iodide (PI) Apoptosis Detection Kit (Dalian Meilun Biotechnology, China). We added appropriate volumes of working solution to the cell pellet, resuspended the cells, and reconstituted the cells at a density of 1×10^6 cells/mL. Next, we pipetted 100 μL of cell suspension (1×10^5 cells) into a new tube, added both Annexin V-FITC and PI (5 μL), and incubated at room temperature for 15 min. Lastly, 400 μL of the working solution was added to each tube, and the level of fluorescence was detected by flow cytometry (BD LSR Fortessa X-20, BD, USA). FlowJo software was used to analyze the data.

Wound healing assay

The cells were plated on a fibronectin-coated 6-well plate. After complete attachment, a vertical scratch was made at the bottom of the well with a 10 μL pipette tip. After washing the cells three times with PBS, a complete medium containing different concentrations of JAS was added to each well. The cells were cultured in an incubator at 37 °C, under 5% CO_2. Images of cells were collected using an inverted microscope (1MT-2-21, Olympus, Japan) and quantified with the ImageJ software.

Transwell assay

We suspended the cells in growth medium without FBS, added 100 μL of the cell suspension to the upper chamber, and then added medium (20% FBS) with different concentrations of JAS to the lower chamber. After 24 hours, cells were fixed in 4% paraformaldehyde for 10 min and stained with 0.1% crystal violet (crystal violet-citric acid staining solution, Soleil, China) for 30 min. Images were obtained with an Olympus microscope.

Alkaline phosphatase activity

Cells were washed three times with PBS and permeabilized with 1% Triton X-100 for 30 min. We followed the instructions of the Alkaline Phosphatase Detection Kit (Nanjing Jiancheng Bioengineering, China). The absorbance of each well was measured at 540 nm using a microplate reader (Bio-Rad, USA). The alkaline phosphatase activity in the sample was calculated from the OD value and the protein concentration of the sample.

Alkaline phosphatase staining

Cells were fixed in 4% paraformaldehyde for 10 min, washed three times with PBS, and incubated with ALP staining solution (Alkaline phosphatase staining kit, Beyotime, China) for 30 min, and then washed three times with PBS. An Olympus microscope was used to acquire images.

Alizarin red staining

The cells were fixed in 4% paraformaldehyde for 10 min, washed three times with PBS, and incubated with Alizarin red staining solution at room temperature for 3 min. Cells were then washed three times with PBS. An Olympus microscope was used to acquire images.

Western blotting

The total protein samples were extracted according to the kit instructions (Whole Protein Extraction Kit, Beyotime, China). The protein was separated by SDS-PAGE (voltage of 80/120 V) and transferred to PVDF membranes at a voltage of 60 V for 3 h. The membranes were blocked with 5% nonfat dry milk for 1 h at room temperature, incubated with primary antibody: GAPDH (1:8000, Cell Signaling Technology, USA); β-actin (1:1000, Bioworld, China); OPN (1:1000, Abcam, USA); RUNX2 (1:1000, Abcam, USA); FAK (1:500, Cell Signaling Technology, USA); Talin (1:1000, Millipore, USA); Vinculin (1:1000, Sigma- Aldrich, USA); Paxillin (1:1000, Becton Dickinson and Company, USA); Zyxin (1:700, Affinity, USA) overnight at 4 ºC with gentle shaking, and incubated with appropriate secondary antibodies: horseradish peroxidase-labeled goat anti-rabbit IgG (H + L) (1:5000, Fdbio Science, China); horseradish peroxidase-labeled goat anti-rabbit IgG (H + L) (1:5000, Fdbio science, China) at room temperature for 1 h. Protein expression was visualized using an exposure instrument (Tanon 5500, Tanon, China). Quantification of western blot data was performed by Gel-pro software.

Statistical analysis

All experiments were repeated at least three times. All values are expressed as mean ± standard deviation (Mean ± SD). All data were statistically analyzed using GraphPad software, a t-test was used for comparison between the two groups, and ANOVA was used for comparison between multiple groups. $P < 0.05$ was considered to indicate statistically significant results.

Abbreviations

hASCs
human adipose-derived stem cells; CCK-8:Cell Counting Kit-8; JAS:jasplakinolide; FAK:focal adhesion kinase; YAP:YES associated protein; ALP:alkaline phosphatase; OPN:osteopontin; RUNX2:Runt-related transcription factor 2; PBS:phosphate-buffered saline; DMSO:Dimethyl sulfoxide; FITC:Fluorescein Isothiocyanate; PI:Propidium Iodide;

Declarations

Acknowledgments

The authors thank Dr. Feng Lu (Southern Medical University, Guangzhou, China) for help in providing human fat tissue.

Funding

This study was financially supported by the National Key R&D Program of China (2017YFC1105000).

Availability of data and materials

All the supporting data can be downloaded.

Ethics approval

This study was approved by the Ethics Committee of School of Basic Medical Sciences, Southern Medical University.

Consent for publication

Not applicable.

Conflict of Interest

The authors declare no conflict of interest.

Author contributions

JO and JD conceived and designed the experiments. BS, TF, RQ, YY, XJ, AUK, and ZZ performed the experiments. BS, TF, and RQ analyzed the data. TF and JD draftedthe manuscript.

References

1. Chugh P, Paluch EK. The actin cortex at a glance. J Cell Sci. 2018;131.
2. Svitkina T. The Actin Cytoskeleton and Actin-Based Motility. Cold Spring Harb Perspect Biol. 2018;10:a018267.
3. Peckham M. How myosin organization of the actin cytoskeleton contributes to the cancer phenotype. Biochem Soc Trans. 2016;44:1026–34.
4. Blanchoin L, Boujemaa-Paterski R, Sykes C, Plastino J. Actin dynamics, architecture, and mechanics in cell motility. Physiol Rev. 2014;94:235–63.
5. Pollard TD, Cooper JA. Actin, a central player in cell shape and movement. Science. 2009;326:1208–12.
6. Bezanilla M, Gladfelter AS, Kovar DR, Lee W. Cytoskeletal dynamics: a view from the membrane. J Cell Biol. 2015;209:329–37.
7. Vicente-Manzanares M, Ma X, Adelstein RS, Horwitz AR. Non-muscle myosin II takes centre stage in cell adhesion and migration. Nat Rev Mol Cell Biol. 2009;10:778–90.
8. Matsubayashi Y, Coulson-Gilmer C, Millard TH. Endocytosis-dependent coordination of multiple actin regulators is required for wound healing. J Cell Biol. 2015;210:419–33.
9. Seixas AI, Azevedo MM, Paes DFJ, Fernandes D, Mendes PI, Relvas JB. Evolvability of the actin cytoskeleton in oligodendrocytes during central nervous system development and aging. Cell Mol Life Sci. 2019;76:1–11.
10. Schmit AC, Lambert AM. Microinjected fluorescent phalloidin in vivo reveals the F-actin dynamics and assembly in higher plant mitotic cells. Plant Cell. 1990;2:129–38.
11. Shoji K, Ohashi K, Sampei K, Oikawa M, Mizuno K. Cytochalasin D acts as an inhibitor of the actin–cofilin interaction. Biochem Bioph Res Co. 2012;424:52–7.
12. McBeath R, Pirone DM, Nelson CM, Bhadriraju K, Chen CS. Cell Shape, Cytoskeletal Tension, and RhoA Regulate Stem Cell Lineage Commitment. Dev Cell. 2004;6:483–95.
13. Fabian I, Halperin D, Lefter S, Mittelman L, Altstock RT, Seaon O, et al. Alteration of actin organization by jaspamide inhibits ruffling, but not phagocytosis or oxidative burst, in HL-60 cells and human monocytes. Blood. 1999;93:3994–4005.
14. Shurety W, Stewart NL, Stow JL. Fluid-phase markers in the basolateral endocytic pathway accumulate in response to the actin assembly-promoting drug Jasplakinolide. Mol Biol Cell. 1998;9:957–75.
15. Terada Y, Simerly C, Schatten G. Microfilament stabilization by jasplakinolide arrests oocyte maturation, cortical granule exocytosis, sperm incorporation cone resorption, and cell-cycle progression, but not DNA replication, during fertilization in mice. Mol Reprod Dev. 2000;56:89–98.
16. Terracciano S, Bruno I, D Amico E, Bifulco G, Zampella A, Sepe V, et al. Synthetic and pharmacological studies on new simplified analogues of the potent actin-targeting Jaspamide. Bioorgan Med Chem. 2008;16:6580–8.

17. Braekman JC, Daloze D, Moussiaux B. Jaspamide from the marine sponge Jaspamide from the marine sponge Jaspis johnstoni. 1987;50:994–5.
18. Zabriskie MT, Klocke JA, Ireland CM, Marcus AH, Molinski TF. Jaspamide, a Modified Peptide from a Jaspis Sponge. 1986;108:3123–4.
19. Crews P, Manes LV, And Boehler M. Jasplakinolide, a cyclodepsipeptide from the marine sponge Jaspis sp. 1986;27:2797–800.
20. Bubb MR, Senderowicz AM, Sausville EA, Duncan KL, Korn ED. Jasplakinolide, a cytotoxic natural product, induces actin polymerization and competitively inhibits the binding of phalloidin to F-actin. J Biol Chem. 1994;269:14869.
21. Matthews JB, Smith JA, Hrnjez BJ. Effects of F-actin stabilization or disassembly on epithelial Cl-secretion and Na-K-2Cl cotransport. Am J Physiol. 1997;272:C254.
22. Hagiwara A, Tanaka Y, Hikawa R, Morone N, Kusumi A, Kimura H, et al. Submembranous septins as relatively stable components of actin-based membrane skeleton. Cytoskeleton. 2011;68:512–25.
23. Van Goor D, Hyland C, Schaefer AW, Forscher P. The role of actin turnover in retrograde actin network flow in neuronal growth cones. Plos One. 2012;7:e30959.
24. Tholpady SS, Llull R, Ogle RC, Rubin JP, Futrell JW, Katz AJ. Adipose tissue: stem cells and beyond. Clin Plast Surg. 2006;33:55–62.
25. Gimble JM, Guilak F, Bunnell BA. Clinical and preclinical translation of cell-based therapies using adipose tissue-derived cells. Stem Cell Res Ther. 2010;1:19.
26. Zuk PA, Zhu M, Mizuno H, Huang J, Futrell JW, Katz AJ, et al. Multilineage cells from human adipose tissue: implications for cell-based therapies. Tissue Eng. 2001;7:211–28.
27. Rodriguez AM, Elabd C, Amri EZ, Ailhaud G, Dani C. The human adipose tissue is a source of multipotent stem cells. Biochimie. 2005;87:125–8.
28. Mesimaki K, Lindroos B, Tornwall J, Mauno J, Lindqvist C, Kontio R, et al. Novel maxillary reconstruction with ectopic bone formation by GMP adipose stem cells. Int J Oral Maxillofac Surg. 2009;38:201–9.
29. Bayati V, Sadeghi Y, Shokrgozar MA, Haghighipour N, Azadmanesh K, Amanzadeh A, et al. The evaluation of cyclic uniaxial strain on myogenic differentiation of adipose-derived stem cells. Tissue Cell. 2011;43:359–66.
30. Stromps JP, Paul NE, Rath B, Nourbakhsh M, Bernhagen J, Pallua N. Chondrogenic differentiation of human adipose-derived stem cells: a new path in articular cartilage defect management? Biomed Res Int. 2014;2014:740926.
31. Yilgor HP, Cook CA, Hutton DL, Goh BC, Gimble JM, DiGirolamo DJ, et al. Biophysical cues enhance myogenesis of human adipose derived stem/stromal cells. Biochem Biophys Res Commun. 2013;438:180–5.
32. Sheykhhasan M, Qomi RT, Ghiasi M. Fibrin Scaffolds Designing in order to Human Adipose-derived Mesenchymal Stem Cells Differentiation to Chondrocytes in the Presence of TGF-beta3. Int J Stem

Cells. 2015;8:219–27.
33. McIntosh K, Zvonic S, Garrett S, Mitchell JB, Floyd ZE, Hammill L, et al. The immunogenicity of human adipose-derived cells: temporal changes in vitro. Stem Cells. 2006;24:1246–53.
34. Bamburg JR, Wiggan OP. ADF/cofilin and actin dynamics in disease. Trends Cell Biol. 2002;12:598–605.
35. Svitkina T. The Actin Cytoskeleton and Actin-Based Motility. Csh Perspect Biol. 2018;10:a18267.
36. Belgardt E, Steinberg T, Husari A, Dieterle MP, Hülter-Hassler D, Jung B, et al. Force-responsive Zyxin modulation in periodontal ligament cells is regulated by YAP rather than TAZ. Cell Signal. 2020;72:109662.
37. Yamashiro Y, Thang BQ, Ramirez K, Shin SJ, Kohata T, Ohata S, et al. Matrix mechanotransduction mediated by thrombospondin-1/integrin/YAP in the vascular remodeling. Proc Natl Acad Sci U S A. 2020;117:9896–905.
38. Yamamoto-Fukuda T, Akiyama N, Kojima H. L1CAM-ILK-YAP mechanotransduction drives proliferative activity of epithelial cells in middle ear cholesteatoma. The American journal of pathology. 2020.
39. Ye G, Li C, Xiang X, Chen C, Zhang R, Yang X, et al. Bone Morphogenetic Protein-9 Induces PDLSCs Osteogenic Differentiation through the ERK and p38 Signal Pathways. Int J Med Sci. 2014;11:1065–72.
40. Li L, Dong Q, Wang Y, Feng Q, Zhou P, Ou X, et al. Hedgehog signaling is involved in the BMP9-induced osteogenic differentiation of mesenchymal stem cells. Int J Mol Med. 2015;35:1641–50.
41. Gu H, Huang Z, Yin X, Zhang J, Gong L, Chen J, et al. Role of c-Jun N-terminal kinase in the osteogenic and adipogenic differentiation of human adipose-derived mesenchymal stem cells. Exp Cell Res. 2015;339:112–21.
42. Sen B, Uzer G, Samsonraj RM, Xie Z, McGrath C, Styner M, et al. Intranuclear Actin Structure Modulates Mesenchymal Stem Cell Differentiation. Stem Cells. 2017;35:1624–35.

Figures

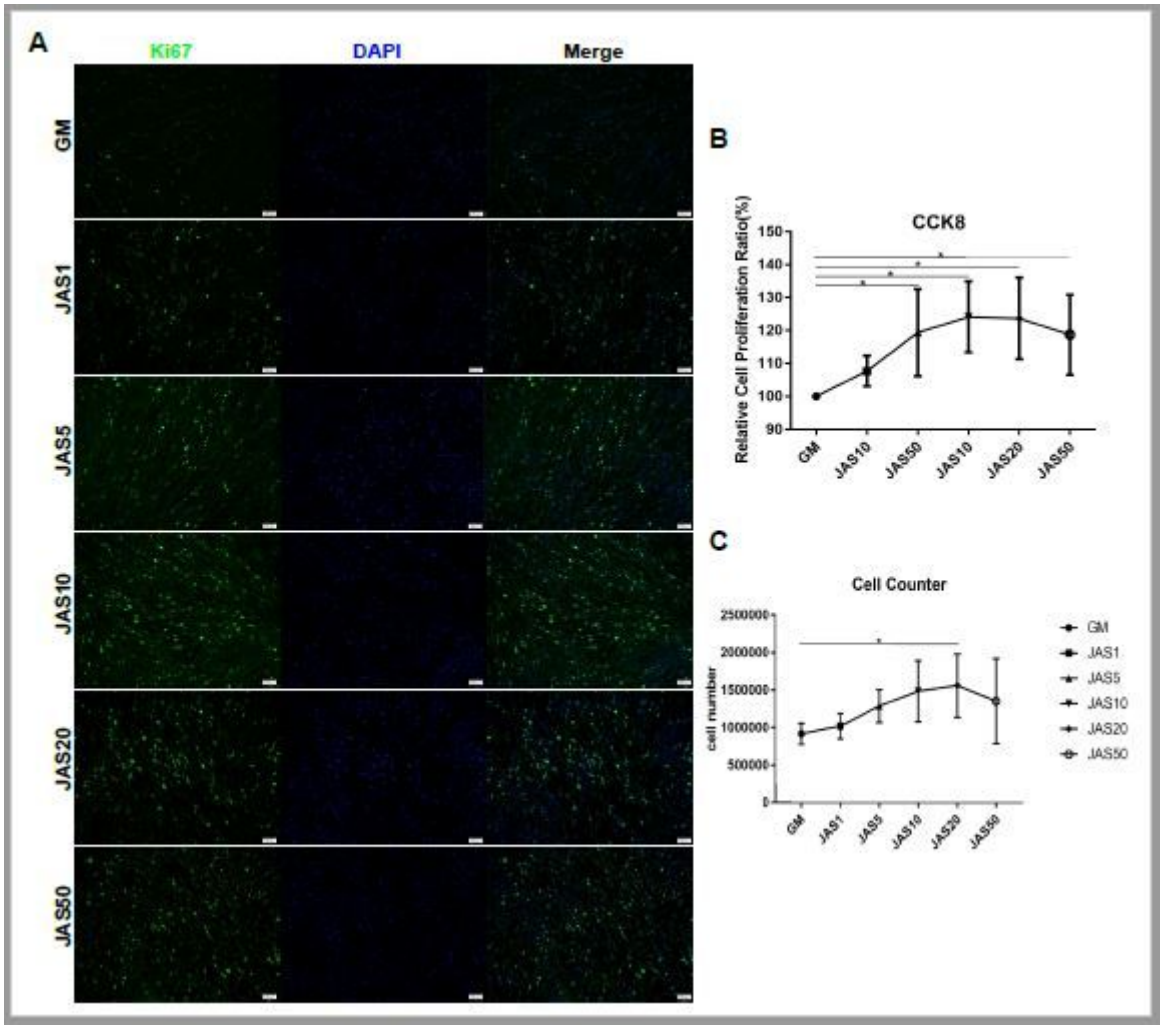

Figure 1

The effect of different actin polymerization states on the proliferation of hASCs. (A) Control and JAS-treatedhASCs stained with Ki67 (green) at day 7. Quantification of the Ki67 positive rate was performed using ImageJ; (B) CCK-8 analysis of hASCs after treatment with JAS for 7 days. Absorbancewas measured at 540 nm; (C) Cell number was obtained using a blood cell count plate. Results are expressed as mean ± SD; *p<0.05. Scale bar = 200 μm.

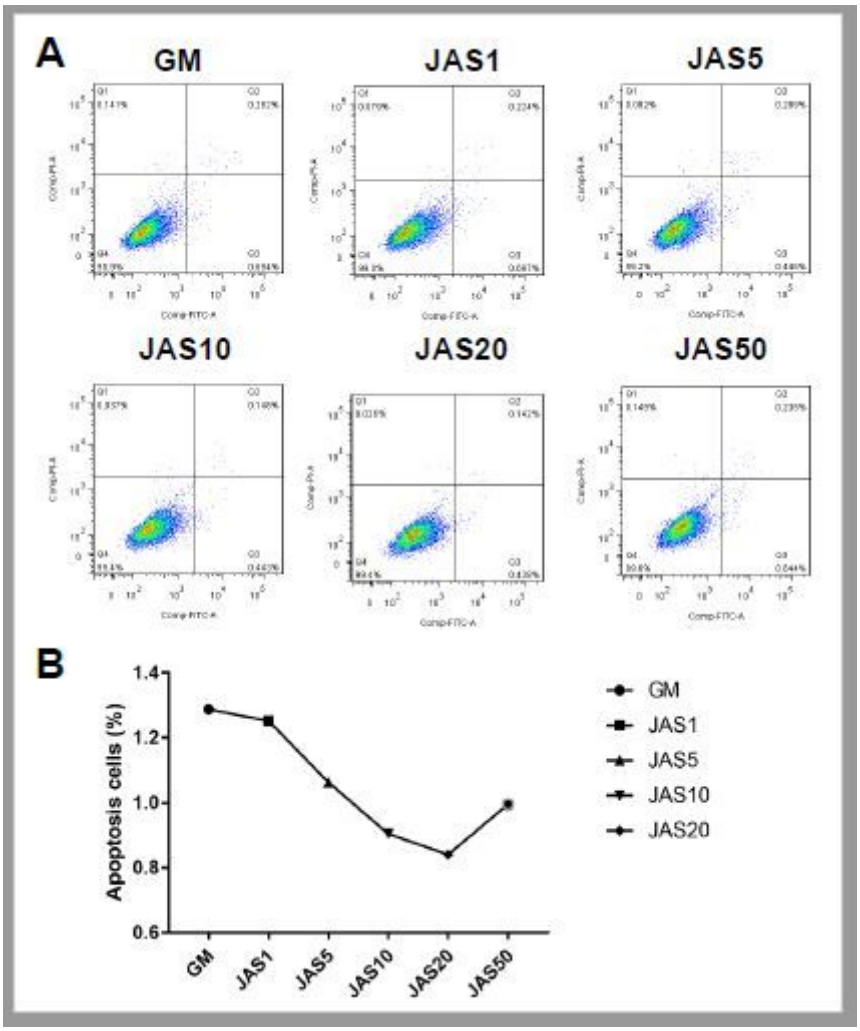

Figure 2

Flow cytometry analysis of the effects of different actin polymerization states on hASCsapoptosis. Cell apoptosis was examined by Annexin V-FITC/PI staining. hASCs were treated with JAS for 7 days, and the expression of fluorescence was detected using flow cytometry and analyzed with FlowJo.

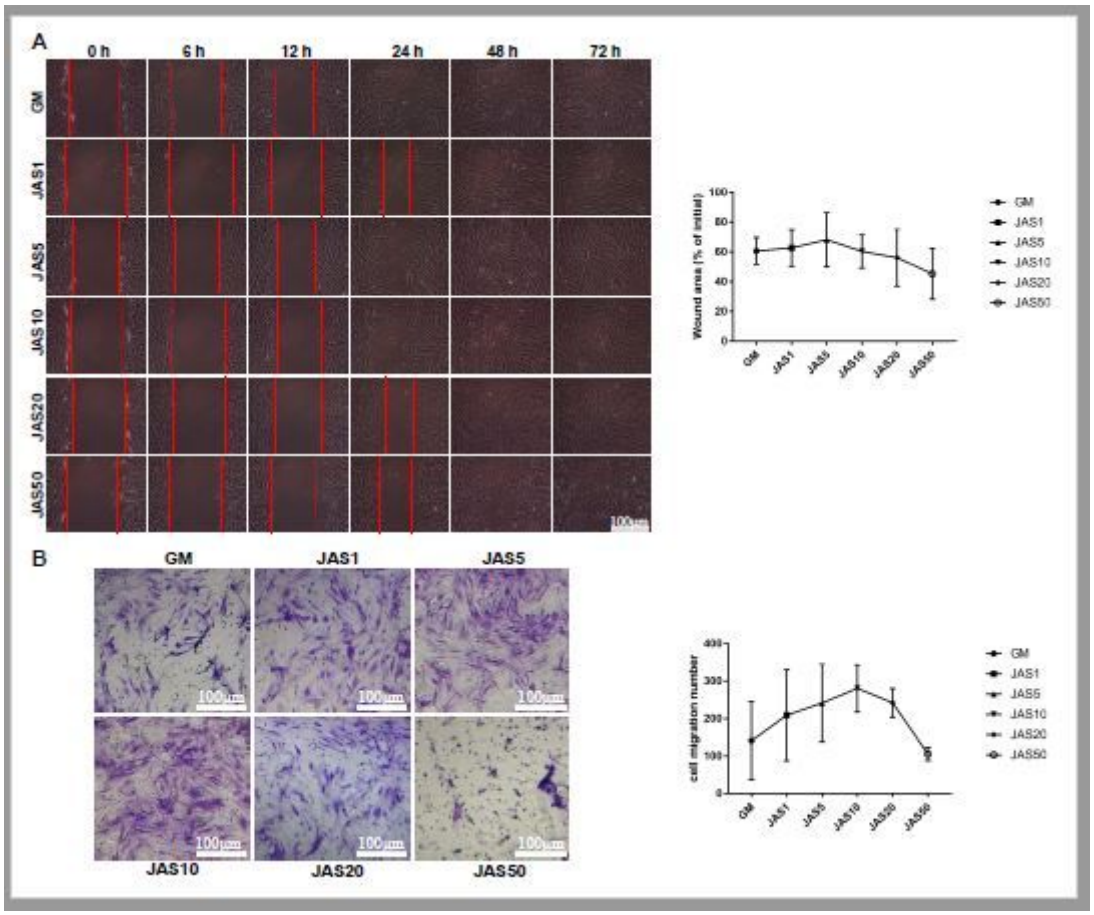

Figure 3

The influence of different actin aggregation states on hASC migration. (A) hASCs were plated on a fibronectin-coated 6-well plate. When cells were completely attached to the plate, confluent monolayers were scratched, and images were captured by microscopy at 0, 6, 12, 24, and 48 h after the scratch. Quantification of the wound area at 0 and 24 h was performed using Image J. The wound area was calculated as the percentage of the initial wound area (0 h). (B) We suspended the cells in complete medium without FBS, added 100 μL of the cell suspension to the Transwell chamber, and then added medium (20% FBS)with different concentrations of JAS to the lower chamber. After 24h, cells were stained with 0.1% crystal violet, and cell counting was performed using Image J. Results are expressed as mean ± SD; *p<0.05. Scale bar = 100 μm.

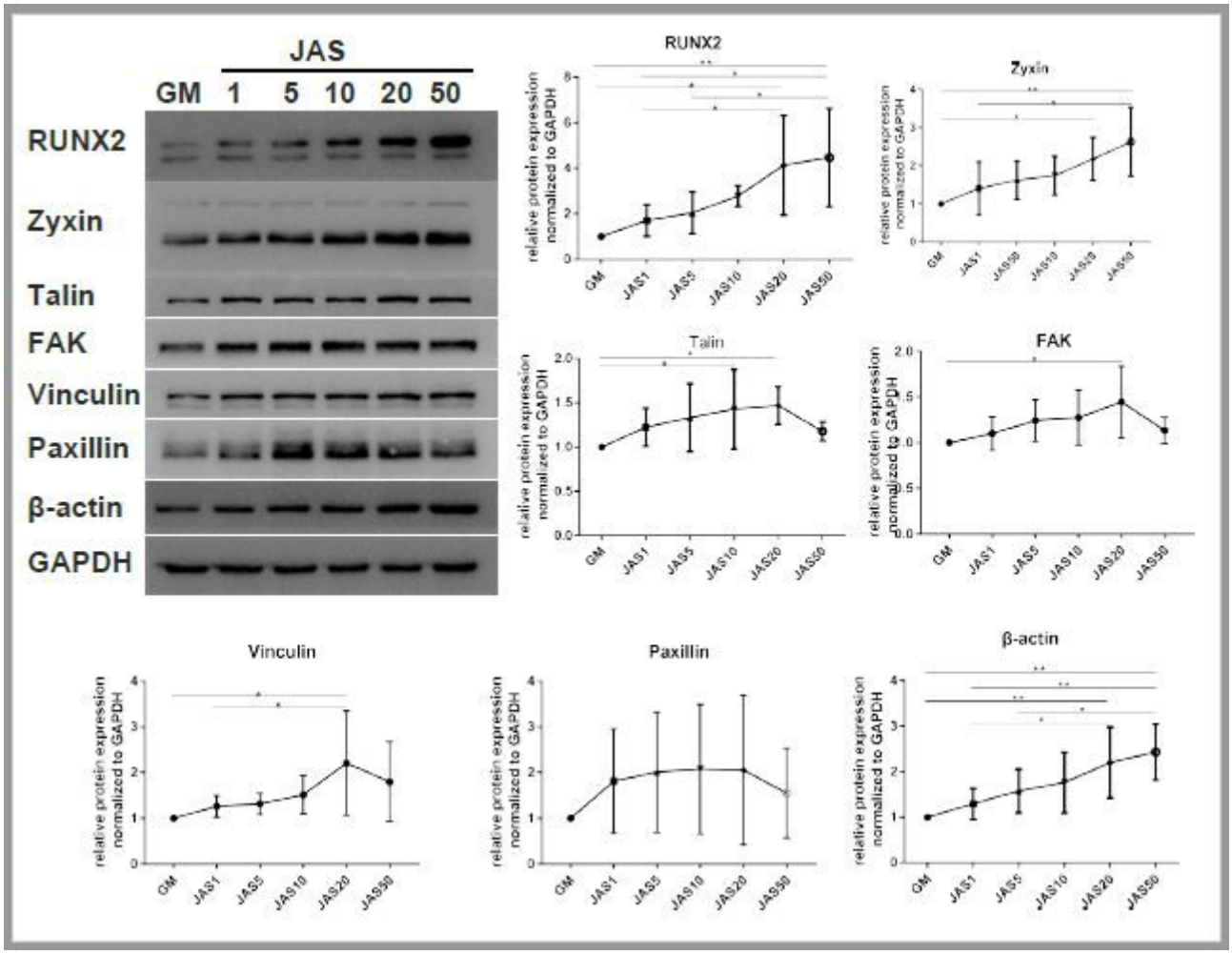

Figure 4

Different actin polymerization states and the maturity of focal adhesions. Western blot analysis was performed to assess the changes in focal adhesion-related proteins of hASCs cultured in medium containing different concentrations of JAS. Samples were collected after 1 week in culture. Quantification of western blot data was performed by Gel-pro software. The relative expression of these proteins was normalized to that of GAPDH. Results are expressed as mean ± SD; *p<0.05.

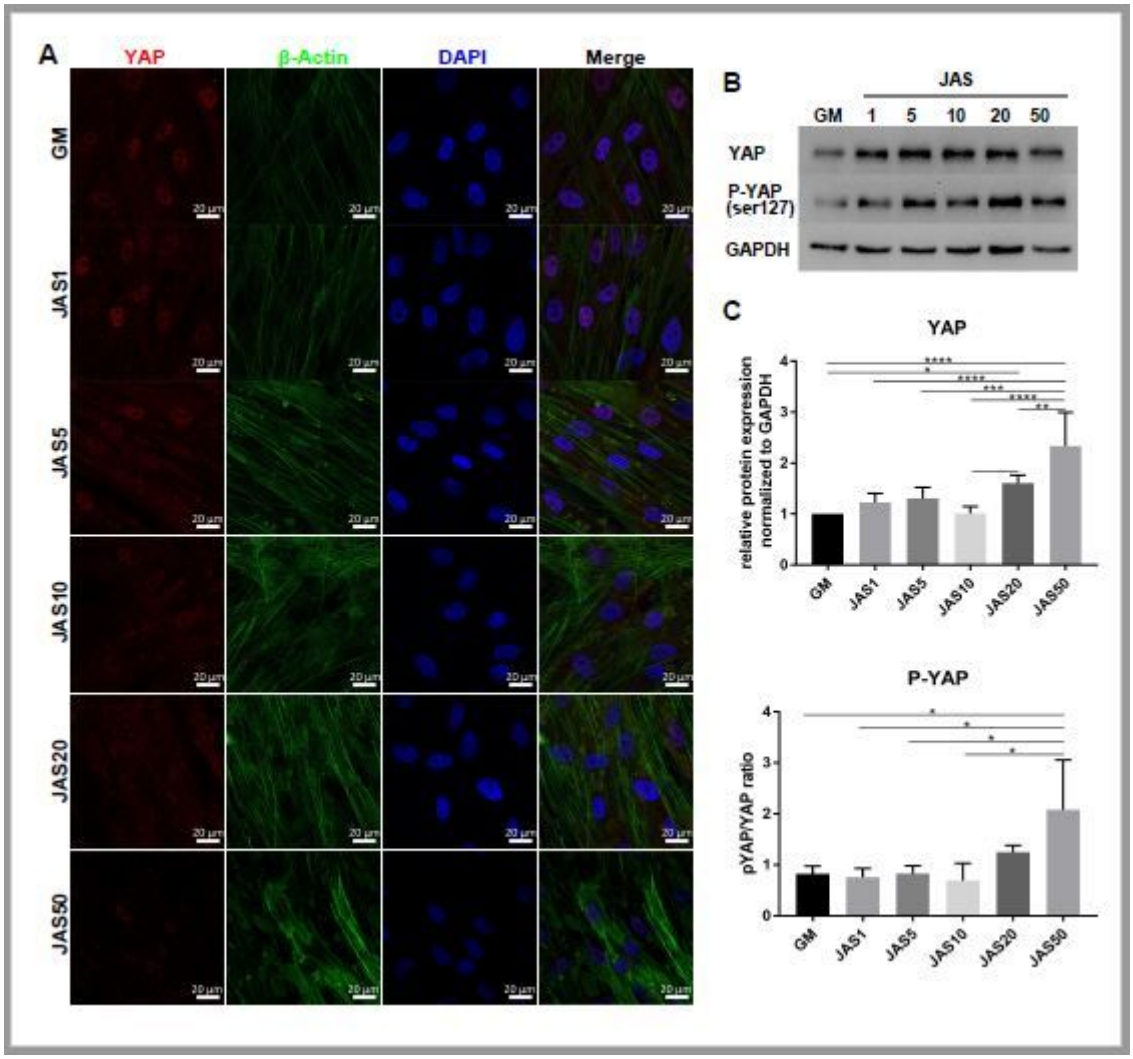

Figure 5

Actin polymerization can promote the localization of YAP protein to the cytoplasm. (A) Cells were cultured inmedium containing different concentrations of JAS. Then, cells were fixed and immunostained with anti-YAP antibodies. Fluorescence for YAP and actin is shown in red and green, respectively. Nuclear staining is represented in blue. All images were obtained using a 63× oil immersion lens on the confocal microscope,Scale bar = 20 μm; (B)Western blot analysis for YAP and p-YAP (Ser127) of hASCs cultured in medium containing different concentrations of JAS; (C)The relative expression of YAP and p-YAP (Ser127) was normalized to that of GAPDH. Results are expressed as mean ± SD; *p<0.05.

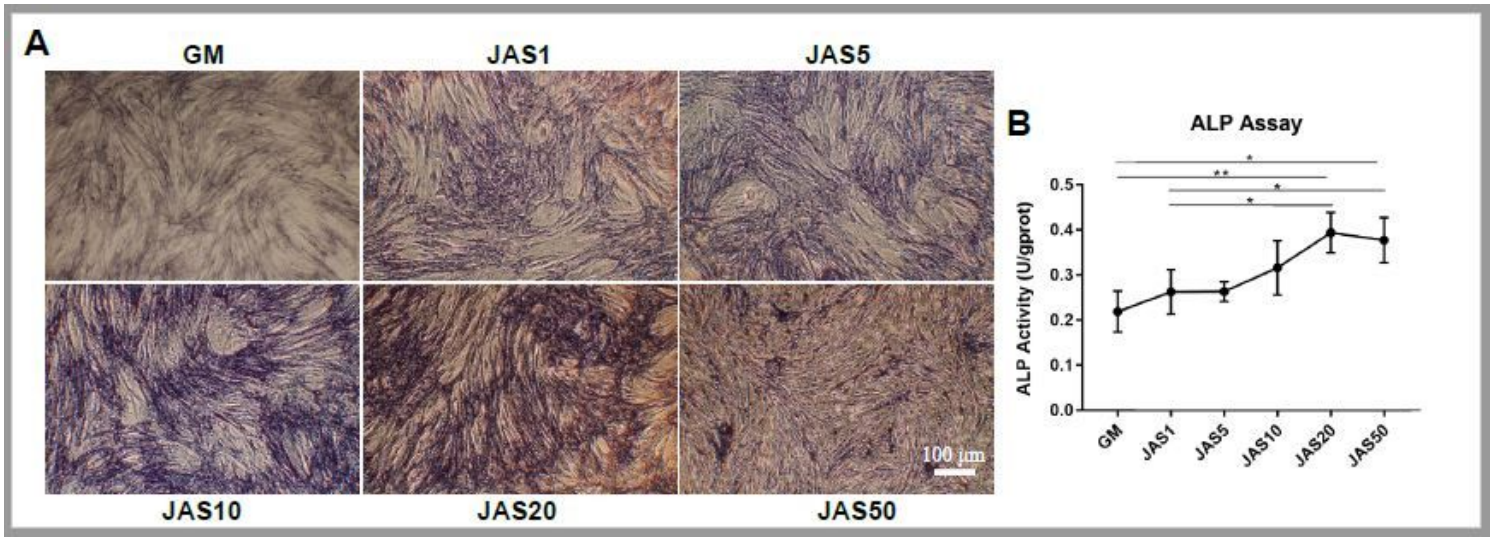

Figure 6

The effects of different actin polymerization states on ALP activity in hASCs. (A) ALP staining of hASCs after treatment with JAS for 7 days; (B) Analysis of ALPactivity of hASCs after treatment with JAS for 7 days. Values are mean ± SD; *p<0.05. Scale bar = 100 μm.

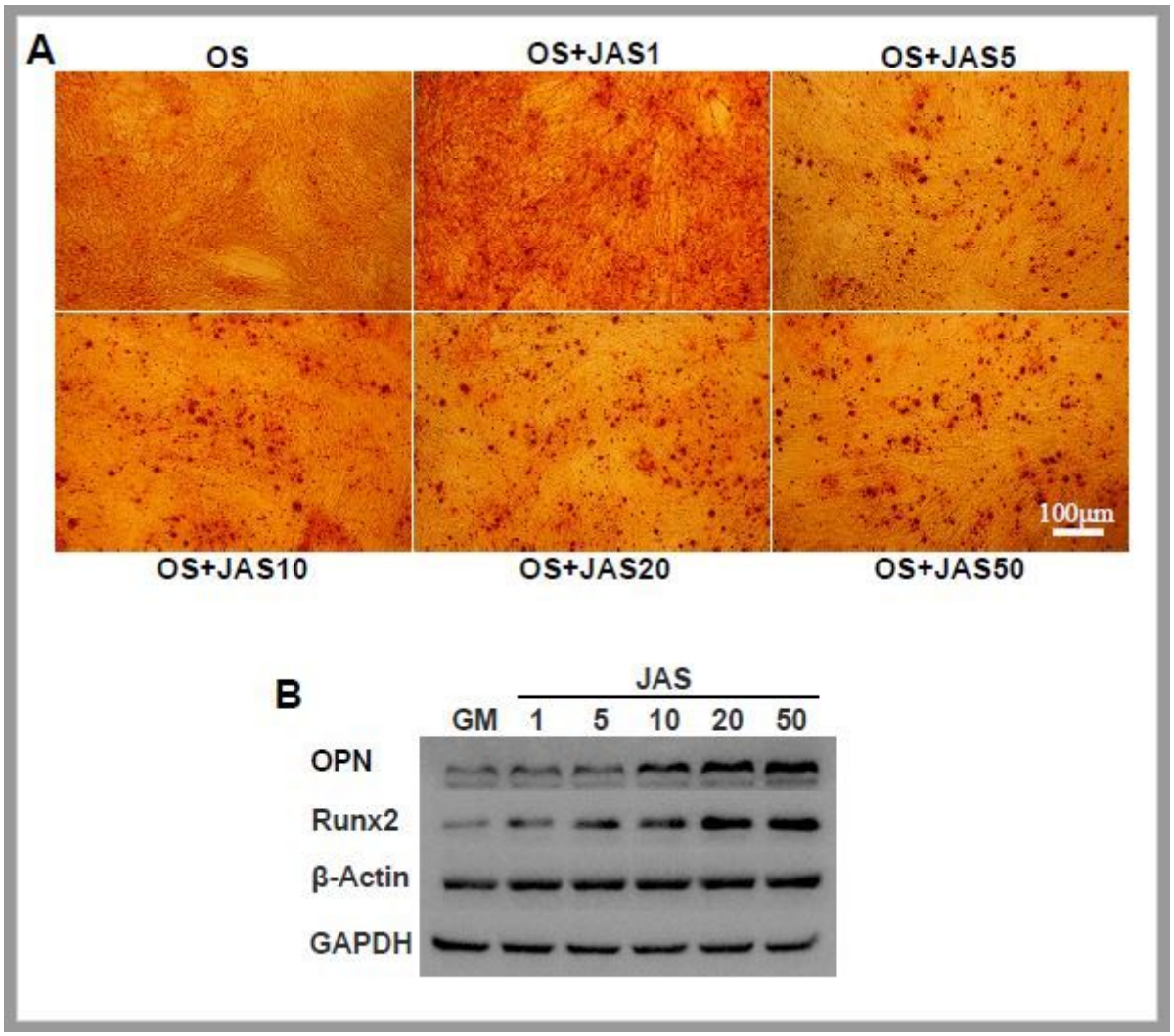

Figure 7

Actin polymerization state and osteogenic differentiation of hASCs. (A) Cells were treated with osteogenic induction medium (containing different concentrations of JAS). They were then stained with alizarin red. Scale bar = 100 μm. (B) Western blot analysis for osteogenic markers of hASCs cultured in the osteogenic induction medium (containing different concentrations of JAS). Samples were collected after one week in culture. Quantification of western blot data was performed by Gel-pro software. The relative expression of these proteins was normalized to that of GAPDH. Values are mean ± SD; *$p<0.05$.